Master's Thesis of Engineering

Design and Study of Hybrid Actuator using Smart Soft Composite and Ionic Polymer-Metal Composite

지능형 연성 복합재와 이온성 고분자-금속 복합체를 이용한 하이브리드 구동기의 설계와 연구

February 2018

Graduate School of Seoul National University
College of Engineering
Department of Mechanical & Aerospace Engineering

Jin Woo Oh

Design and Study of Hybrid Actuator using Smart Soft Composite and Ionic Polymer-Metal Composite

Advisor Prof. Sung-Hoon Ahn

Submitting a Master's Thesis of Engineering

October 2017

Graduate School of Seoul National University
College of Engineering
Department of Mechanical & Aerospace Engineering

Jin Woo Oh

Confirming the master's thesis written by
Jin Woo Oh

December 2017

Chair	이 건 우	(Seal)
Vice Chair	안 성 훈	(Seal)
Examiner	박 용 래	(Seal)

Abstract

Design and Study of Hybrid Actuator using Smart Soft Composite and Ionic Polymer-Metal Composite

Jin Woo Oh
Department of Mechanical and Aerospace Engineering
The Graduate School
Seoul National University

The key advantage of soft-bodied robots over conventional hard-bodied robots is that the soft robotic limb can create smooth, organic and complex movements. Among numerous methods of actuation, smart materials with unique properties can be integrated in soft robots to achieve enhanced maneuverability and to substantially decrease body weight. Traditionally, a single material approach has been implemented to strategically accentuate and manipulate the unique properties of the target material for the intended purpose. However, the addition of a second material can alter the functionality or even augment the performance of the original single-material system.

In this research, a hybrid actuator consisting of a shape memory alloy (SMA)-based smart soft composite (SSC) actuator and an ionic-polymer metal composite (IPMC) was designed and manufactured. Two actuators based on distinct materials were

assembled in series, with one serving an assistive role for the other. Taguchi method was used to create an experimental design to test various parameters that affected the hybrid actuator performance. The effect of altering the parameters of the SSC control method was explored by changing the duty cycle of the PWM. Lastly, the assistive role of the IPMC was investigated by evaluating the direct effects of it on the SSC.

Keyword : shape memory alloy (SMA), smart soft composite (SSC), ionic polymer–metal composite (IPMC), smart materials, soft robotics, hybrid actuator
Student Number : 2016–20693

Table of Contents

List of Figures

List of Tables

Chapter 1. Introduction

1.1. Hybrid Actuator of Distinct Mechanisms

Generally, the word "hybrid" refers a new and original system created from the amalgamation of two distinct entities. For many years in the field of soft robotics, most of the research has been focused on the manipulation of a single material or mechanism to achieve a specific goal. The use of a single material simplifies the problem to develop its unique properties into strengths, whilst relying on the design to moderate the impact of its weaknesses on the system. Smart materials, with their unique properties, suggest possibilities of numerous fascinating solutions to engineering problems. Ma *et al.* [1] have proposed the design of a robotic bee with piezoelectric muscles that allow the wings to flap at the high frequency of 120 Hz for aerial movement. Villanueva *et al.* [2] have used the shape memory alloys (SMA) to create a jellyfish robot capable of movement underwater with low actuation frequency. Sunkara *et al.* [3] have created a robotic fish with one caudal and two pectoral fins actuated with ionic polymer–metal composite (IPMC) actuators, taking advantage of the material's enhanced performance in the presence of water. There are countless other robotic systems and actuators that are based on different materials, such as shape memory polymers (SMP) [4–9], photomechanical materials [10–13], and more. However, there is a significant lack of research that attempts to interact multiple materials with distinct mechanisms for a common function in a single system.

Although the general tone of the research in soft robotics actuation leans toward a dismissive tone to go "hybrid," there have been a few instances where multiple materials or actuation mechanisms have been integrated in a single body [14,15,17–20]. Shi *et al.* [14, 15] integrated SMA wires with IPMC actuators in their design to fabricate an amphibian robot that could walk on ground (standing mode) and swim in water (lying mode). The

modes can be switched back and forth with the SMA wires to change the orientation of the IPMC actuators, which serve their purpose as legs or fins according to the mode. A single-material, multi-mechanism system was achieved by Shintake *et al.* [16]. They have created a dielectric elastomer-based soft gripper with electroadhesion capabilities at each limb' s tip to compliant and secure gripping. Other instances of a hybrid actuation system involve integration of parts that have less direct impact on the output due to the stark disparity of their nature and purpose, and thus identify as no more hybrid than the unification of multiple disciplines that come into creating any system one could imagine.

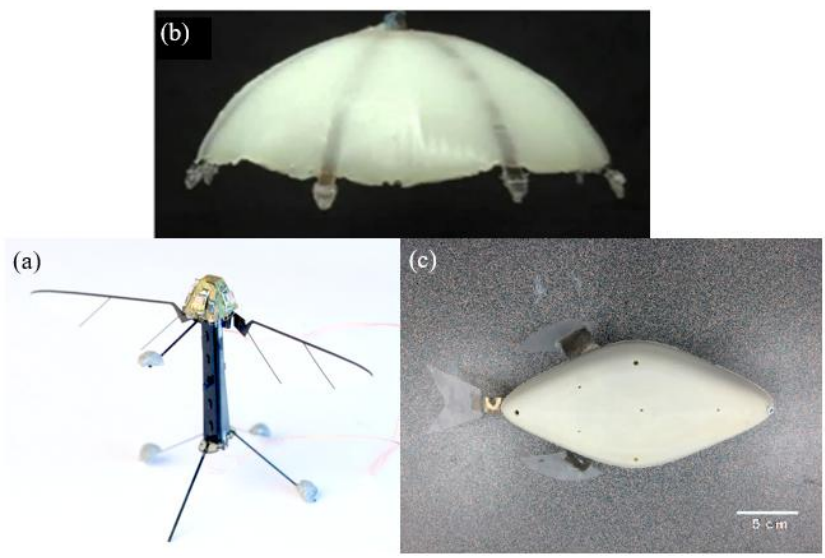

Figure 1.1 Robots made from different smart materials: (a) RoboBee with PZT, (b) jellyfish robot with SMA wires, (c) fish robot with IPMC

Technically, a hybrid actuator can be defined as a body consisting of multiple actuators combined into one, or a single actuator with multiple underlying mechanisms that drive its motion. For the scope of this research, however, a hybrid actuator is defined as that which harbors two or more distinct actuation mechanisms to produce unique movements or modes, potentially creating a characteristic change in performance compared to the

use of only one of the constituent parts. The materials that were considered to explore these traits were the SMA and the IPMC.

1.2. Materials

1.2.1. Shape Memory Alloy (SMA)

The SMA are alloys that are alloys that "remember" their original shape prior to deformation and return to the pre-programmed geometry upon heating to the temperature above their glass transition temperature (T_g) [21, 22]. The most prominent form of SMA is in the form of wires, manufactured and distributed by Dynalloy Inc. While almost all commercially obtained SMA wires are alloys of Nickel and Titanium (55 wt% and 45 wt%, respectively), metallic impurities, such as Palladium is occasionally used to produce SMA with a different T_g. SMA are known for their high force density, but the performance is heavily dependent on the rate of heat dissipation from its structure.

The unique property that allows SMA to recover its original shape is known as *pseudoelasticity*, or *superelasticity* [21]. Upon imposition of stress, the SMA changes its crystalline structure from twinned martensite to deformed martensite. As the increased temperature approaches the alloy's T_g, the martensitic properties begin to disappear. Simultaneously, the austenitic properties become more apparent, while the pre-imposed deformations become undone. Once attaining its austenitic state above T_g, the material can be cooled down again to twinned martensite state, where the structure can be changed again.

Using the SMA wires, Ahn *et al.* [22] proposed the design of a smart soft composite (SSC) actuator. The SSC actuator, with its soft polydimethylsiloxane (PDMS) matrix and a pliable, 3D printed, directional scaffold, is actuated by the activation of SMA wires embedded in its structure. It is capable of both out-of-plane deformation and in-plane deformation, controlled by the pre-

selected directionality of the scaffold. Placement of SMA wires away from the neutral plane and closer to the PDMS surface allows the actuator to deform and bend when the wires are shrunken. To ensure shrinkage, the wires are clamped at the protruding ends with metallic rings that push against the PDMS matrix upon SMA activation.

1.2.2. Ionic Polymer–Metal Composite (IPMC)

IPMC are electroactive polymers that move upon exposure to electrical potential across its structure [24, 25]. It is created by coating precious metals, such as Pt and Au, on both sides of the Nafion polymer sheet, most commonly via electroless plating [26]. The coated sides act as electrodes that allow the electrical potential across the thickness of the actuator to transport water molecules, and cause Coulombian forces to create bulk movements in the actuator. IPMC is capable of high–frequency actuation, but has very low force density. Its performance is also heavily dependent on the moisture content of its structure.

1.3. Purpose of Research

The purpose of this research was to design and fabricate a hybrid actuator consisting of two distinct smart materials: SMA and IPMC. A new design was proposed to match the scales of the two actuators while allowing integration that did not structurally interfere with each other. SSC actuator, with its high force density, was chosen to be the main component, while the IPMC was selected to take on an assistive role in the hybrid actuator. Parameters that affect the performance of the hybrid actuator were evaluated. The effects of the supportive component of IPMC on the SSC was also investigated to determine the characteristic of the hybrid actuator. The potential applications of the hybrid actuator was also examined.

Chapter 2. Design

2.1. Design of Hybrid Actuator

For the integration of two smart materials in a single soft actuator, two designs were initially proposed: serial configuration and parallel configuration. The initial designs were proposed with the intention that each of SSC and IPMC would play a separate role in the overall net movement, and that they would be controlled individually. Due to the disparity in the force scale of the two smart materials, the SSC was designated to be the main actuator, while the IPMC was chosen as a supporting actuator to the SSC component by altering its performances. Furthermore, in order to maximize the effects of the IPMC actuator, a serial configuration was considered such that the moment caused by IPMC at the free end of the SSC would have the greatest effect on the SSC performance. Figure 2.1 shows the proposed design of the hybrid actuator.

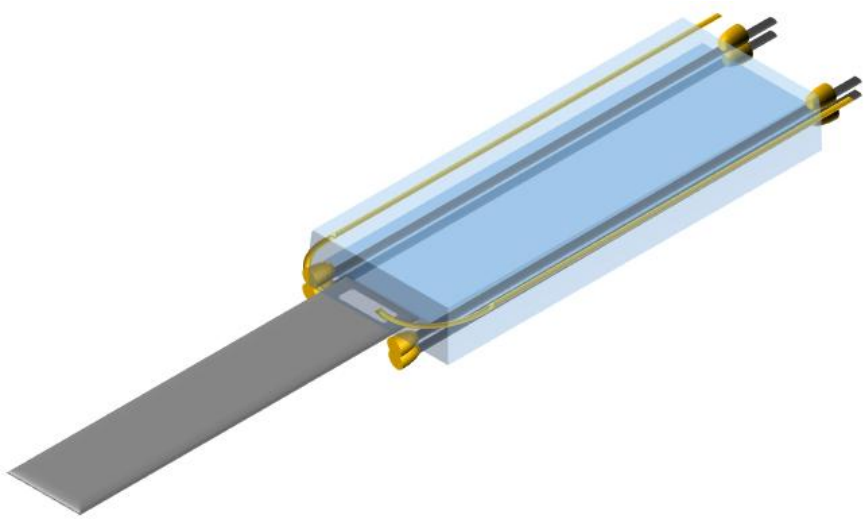

Figure 2.1 Proposed design of the hybrid actuator in serial configuration

2.2. Design of SSC

The design of the SSC actuator was modified from the previous design proposed by Song et al in order to allow for integration of IPMC. Width and thickness were significantly decreased to lessen the influence of air resistance while enhancing heat dissipation rate via convection for improved performance of the embedded SMA wires, as shown by the mold design in Figure 2.2.

Post-curing processes during the fabrication of sample have also been adjusted accordingly. The clamped ends were electrically shorted with silver paste, instead of the traditional application of soldering lead. The primary reason for replacing the conventional soldering method was that the high temperature (ranging from 300 to 320°C) from the liquefied metal caused the PDMS matrix to shrink, weakening its grip around the clamped rings. It is the integrity of the PDMS structure secured tightly around the camped rings that ensure the proper actuation of the SSC actuator. Electrical wires were attached at the free end of the actuator for both upper and lower sides with silver paste to allow connection to a power supply. PDMS was coated over the pasted wires once more to secure connection to the clamped rings and to prevent abrasion of the metal paste.

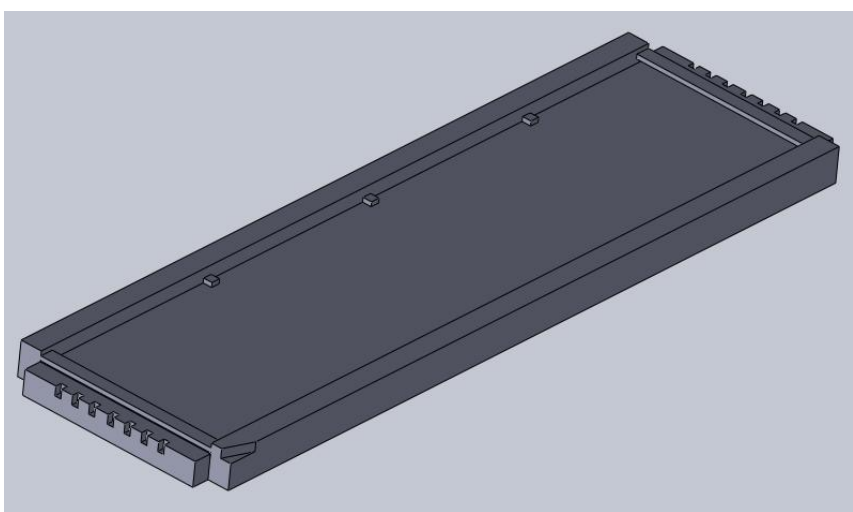

Figure 2.2 Altered mold design for the SSC actuator

Additionally, thin wires were also embedded in the PDMS matrix prior to curing to allow individual control of the IPMC at the tip.

For the experiments, a variation of parameter values was chosen to design the actuator. The width of the SSC actuator was held constant at 20 mm, while two distinct of values were selected each for length (60 mm & 80 mm) and thickness (1.5 mm & 1.7 mm). Mold parts of different sizes and thicknesses were 3D printed.

2.3. Design of IPMC

The cantilever beam form was selected for the design of the IPMC, to maintain the geometrical uniformity with the SSC actuator. The strip of IPMC was prepared in dimensions of 4 mm x 25 mm. Because of the low force density of IPMC, dimensions were kept at constant. The experiments were done with and without the IPMC to simply validate the difference in performance, not the variation in performance from different sizes of IPMC.

Chapter 3. Fabrication

3.1. Fabrication of SSC

In order to create the SSC sample, a mold was first 3D printed with polyactic acid (PLA) to place all the components of the actuator. SMA wires with T_g of 70°C and 0.004 in. diameter were placed above and below the scaffold 3D printed with acrylonitrile butadiene styrene (ABS) within the PLA mold. 100 g weights were tied to each end of the SMA wires to ensure tautness throughout the hardening process. Thin conducting wires were also placed at the sides for independent IPMC control. PDMS polymer with 1:10 epoxy-to-silicon base was carefully poured into the mold to prevent formation of air bubbles within the matrix, as shown in Figure 3.1. The filled mold was placed in the curing oven for about 5 hours at 50°C.

Figure 3.1 Scaffold, SMA wires and regular wires encased in PDMS

After complete hardening of the PDMS matrix, the structure was removed from the mold. The ends of the SMA wires were clamped tightly to the surface of the PDMS body with small metallic rings to ensure highly responsive actuation to the activation of embedded SMA wires. After wires were attached at the four clamped sections on both ends and sides of the SSC actuator, silver paste and PDMS were used to secure the wires. Figure 3.2 shows the finished sample.

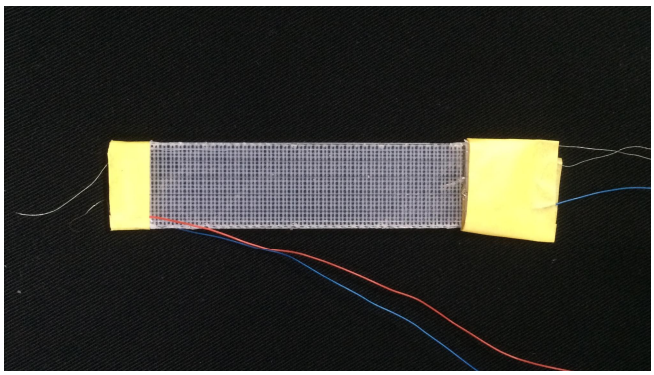

Figure 3.2 SSC actuator

3.2. Fabrication of IPMC

For the fabrication of IPMC, sheets of Nafion 117 were coated with Pt on both sides via chemical plating. Nafion 117 samples were first cut up in sizes of 50 mm x 50 mm and sandpapered on both sides to facilitate impregnation of Pt particles on the surface. The samples were rinsed in distilled water at 100°C for 1 hour, then submerged in 5% sulfuric acid for 1 hour at 80°C. The samples were then placed in a solution of approximately 25% ammonium hydroxide with 100 mg of tetraammineplatinum(II) chloride at 60°C for 9~12 hours so that the Pt^{2+} ions could attach to the surface of Nafion, as shown in Figure 3.3.

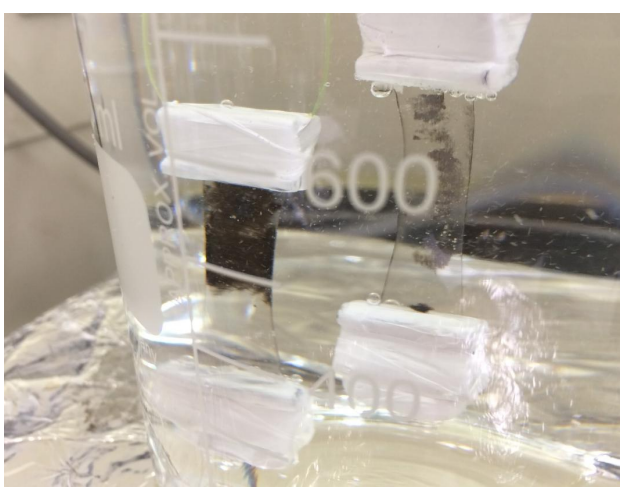

Figure 3.3 Impregnation & reduction of Pt^{2+} ions

Lastly, the Pt^{2+} ions were reduced with a solution of distilled water with 200 mg of sodium borohydride added over 2~3 hours. The steps of Pt impregnation and reduction were repeated for 7~9 times until the surface resistance of the IPMC samples was reduced to about 1~3 Ω (Figure 3.4).

Figure 3.4 Measurement of IPMC surface resistance

After the electroless plating process, the samples were cut up in 4 mm x 25 mm cantilever-shaped strips for testing. Figure 3.5 shows the finished sample.

Figure 3.5 IPMC actuator

3.3. Integration

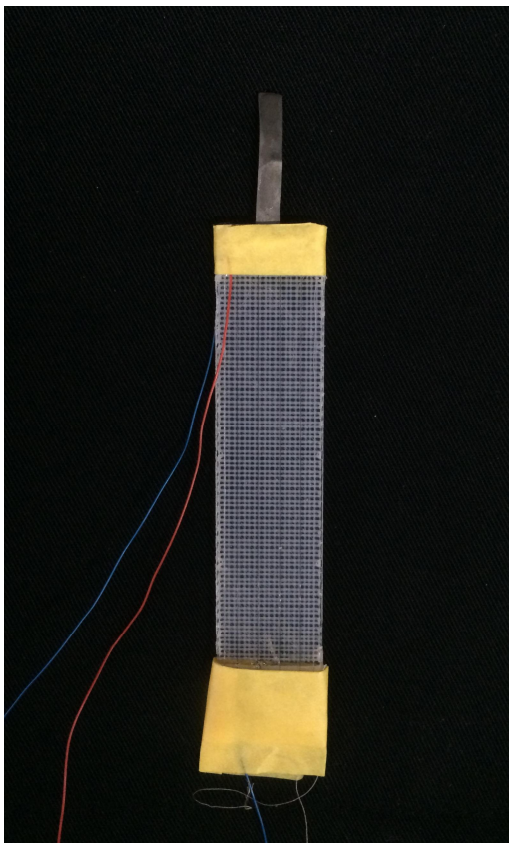

Figure 3.6 Completed sample of hybrid actuator

The SSC and IPMC actuators were combined in serial configuration by attaching the IPMC at the free end of the SSC. The PDMS-coated clamps on the free end of the SSC actuator were first split into upper and lower layers with a surgical knife, and insulated to insert the IPMC actuator. The two thin electrical wires embedded in the PDMS matrix were reconfigured to lead into the open slit, where each wire was connected to each side the IPMC actuator to supply electrical current for actuation. The completed hybrid actuator sample is shown in Figure 3.6.

Table 1 shows the specifications of the completed hybrid actuator and its components for the SSC with four SMA wires on each side.

Table 1. Specifications of SSC, IPMC and hybrid actuator

	SSC	IPMC	Hybrid Actuator
Width	20 mm	5 mm	20 mm
Length	80 mm	25 mm	118 mm
Thickness	1.75 mm	0.2 mm	1.75
Resistance	7.78 Ω	66.7 Ω	–
Voltage	14 V	10 V	–
Current	1.8 A	0.2 A	–
Power Consumption	25.2 W	2 W	27.2 W

Chapter 4. Experimental Design

4.1. Taguchi Method

In order to determine the actuation performance of the hybrid actuator, the Taguchi's design of experiments (DOE) was implemented on the SSC component. The decision to designate the IPMC actuator to take on an assistive role in the hybrid actuator was initially based on the supposed disparity of the actuators' tip forces. The preliminary test results have confirmed a significant difference in force scale between the SSC actuator and IPMC of approximately 29.31 to 1, as shown in Table 2. Because a large portion of the tip force exerted and the bulk movement of the hybrid actuator were mainly produced by the SSC actuator, there was deemed adequate to determine that the performance and behavior of the hybrid actuator followed closely to those of the SSC. Thus, in order to evaluate the characteristics of the hybrid actuator, the Taguchi method was used to examine the various parameters of the SSC actuators.

Table 2. Preliminary test results of actuator force

SSC	IPMC	SSC:IPMC
186.42 mN	6.36 mN	29.31

To apply Taguchi method, the L4 (2^3) orthogonal array was chosen to examine three parameters of the SSC actuator: length, number of SMA wires, and scaffold thickness. As shown in Figure 4.1 and Table 3, each parameter was varied at two distinct values of 60 mm & 80 mm for length, 2 & 4 for number of SMA wires, and 0.5 mm & 0.7 mm for scaffold thickness to examine their effects on the hybrid actuator's angle of deformation, thrust, and resonance frequency. Due to the significant disparity in tip force, the parameters of the IPMC actuator were held constant. With regards

to the IPMC, it was deemed sufficient for the scope of this research to simply validate any effect that IPMC actuator had on the SSC during the activation of both components. The primary interest, however, was in the variation of SSC performance.

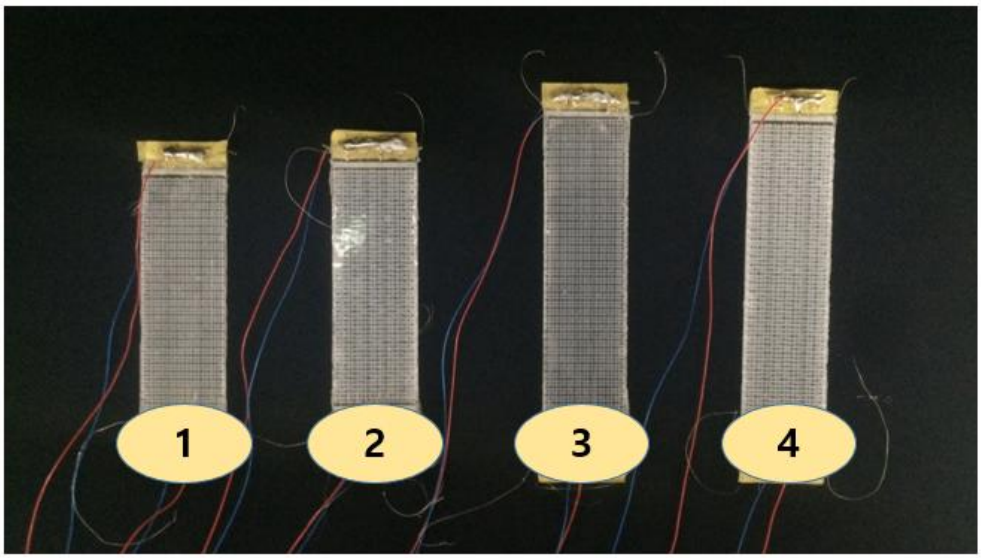

Figure 4.1 SSC actuator samples with variation in parameters (showing samples 1~4, from left to right)

Table 3. Specifications of tested samples

	Sample 1	Sample 2	Sample 3	Sample 4
Length	60 mm	60 mm	80 mm	80 mm
Number of SMA wires	2	4	4	2
Scaffold thickness	0.5 mm	0.7 mm	0.5 mm	0.7 mm
Width	20 mm			
SMA wire thickness	0.1016 mm (0.004 “)			

4.2. Experimental Setup

Two distinct experimental setups were used for the evaluation of

hybrid actuator characteristics. Figure 4.2 shows the setup for the deformation test to examine the range of tip deformations achievable under various levels of voltage. The DC power supply was used in conjunction with the Arduino setup to transmit pulses of set currents at the designated voltage to operate the SSC actuator. The function generator was used to transmit alternating current to the IPMC actuator. The gridded background was used to determine the level of tip deformation. Figure 4.3 shows the setup for the force test to determine the thrust caused by the flapping motion of the actuator. The dynamometer by KISTLER was used with the force sensor the measure the force produced by the actuator. A special jig was mounted on the force sensor to facilitate the measurement of thrust.

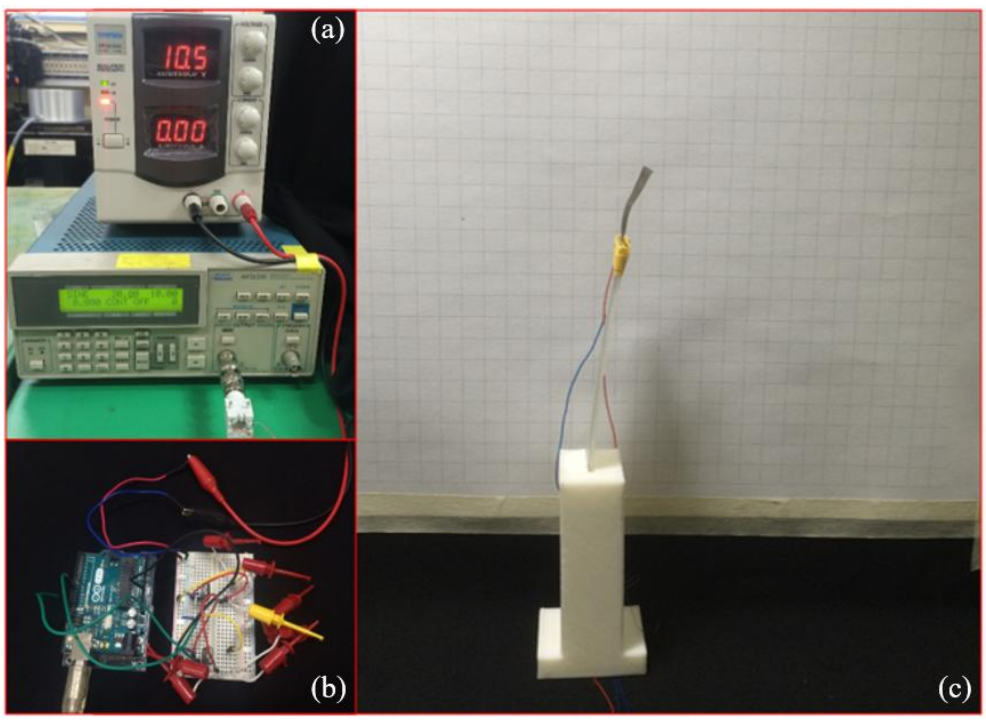

Figure 4.2 Experimental setup for measurement of tip deformation; (a) DC power supply and function generator (top to bottom), (b) Arduino setup used to control inputs of DC current into the SSC actuator, (c) setup of the hybrid actuator on mounting jig

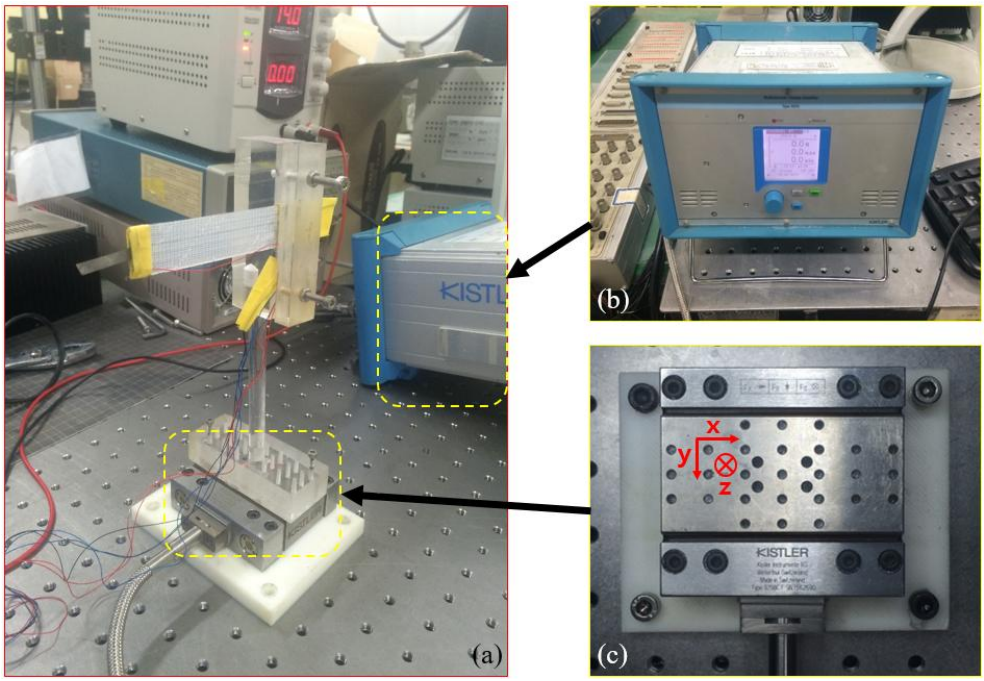

Figure 4.3 Experimental setup for measurement of force; (a) setup of the hybrid actuator on jig for thrust test, (b) dynamometer, (c) force sensor

Chapter 5. Investigation of Parameters

5.1. Actuation and Deformation

One of the most important characteristics that make a limb actuator effective is the extent of deformation it is capable of attaining. Actuation and deformation tests have shown that the hybrid actuator is capable of not only high level of angular deformation, but also capable of taking on nine distinct modes during its actuation. Figure 5.1 shows the nine different modes of actuation that can be observed during the operation of the hybrid actuator. It was observed that the highest levels of angle of deformation by the SSC and IPMC actuators were achieved immediately after short periods of exposure (~2.5 seconds) to DC currents.

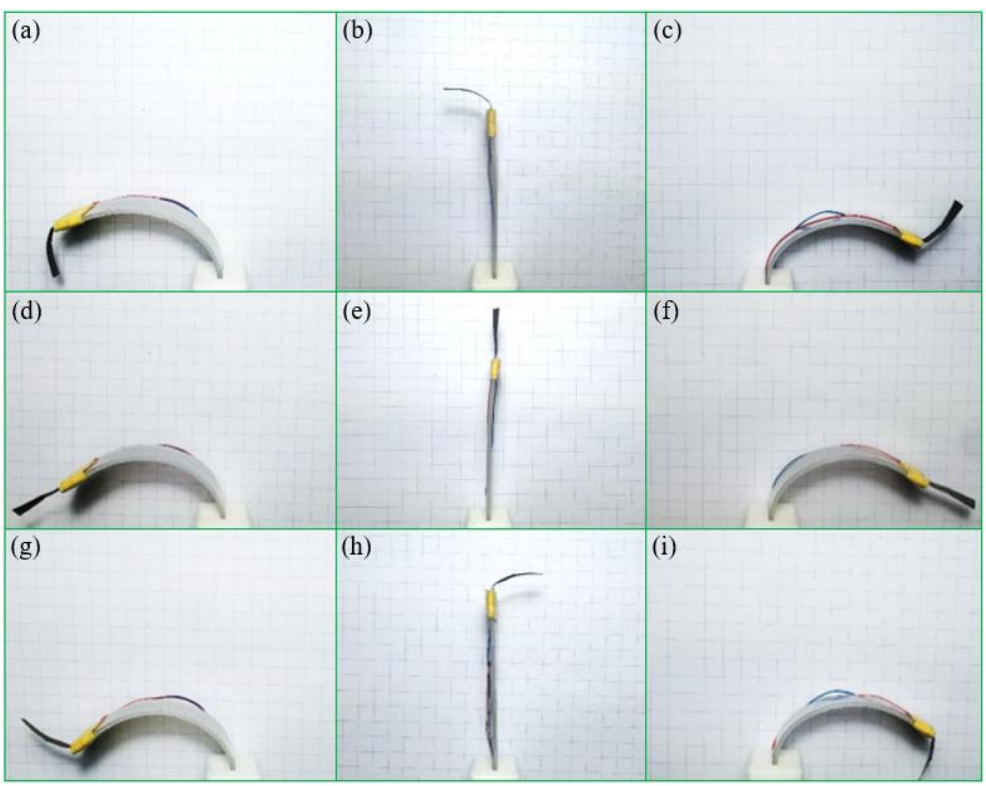

Figure 5.1 Nine modes of actuation achivable by the hybrid actuator

To assess the capabilities of the hybrid actuator, the angular

deformation of its constituent parts were also examined. The plot of Figure 5.2 shows that the IPMC showed increase in angular deformation with increasing current. A constant voltage of 10 V was

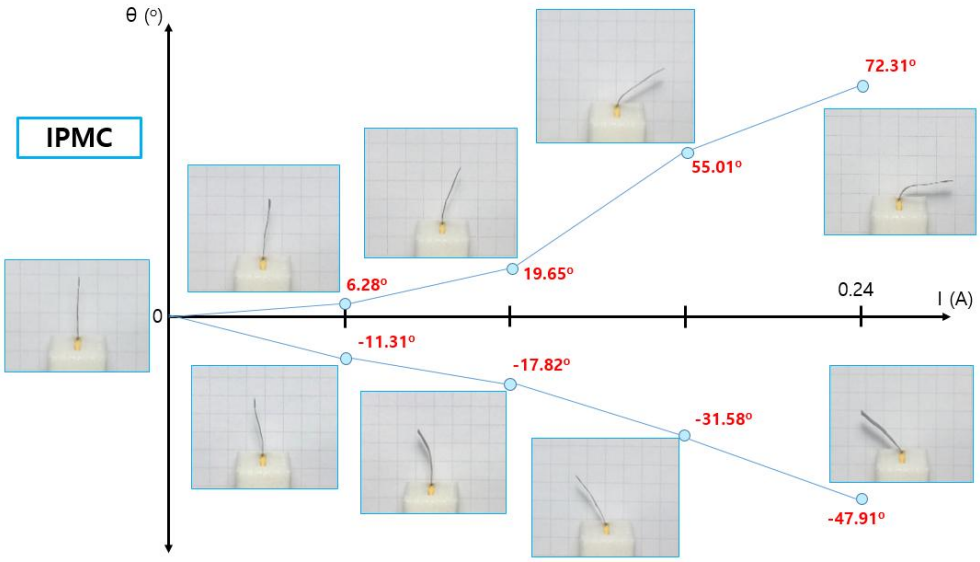

Figure 5.2 Angular deformation vs. current for IPMC

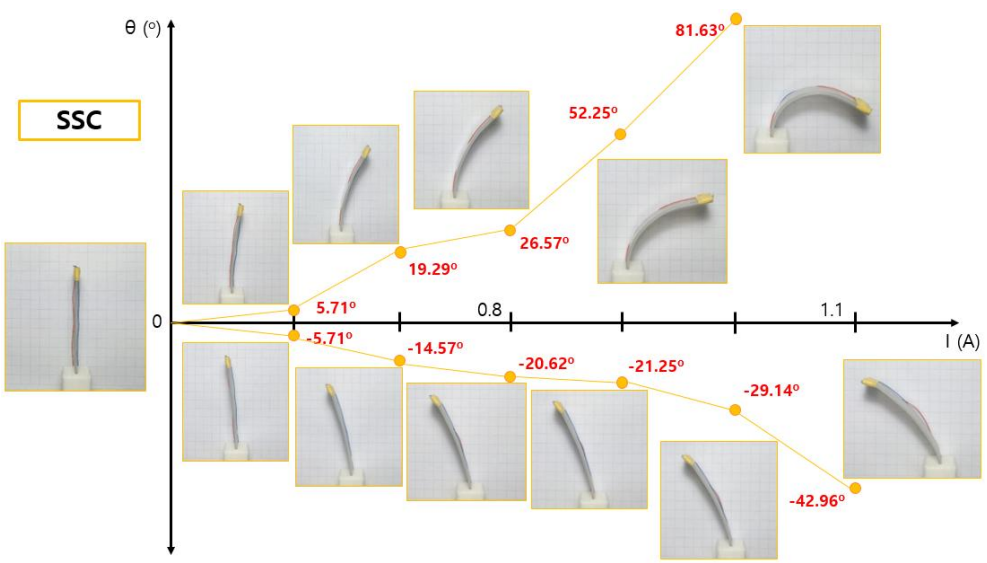

Figure 5.3 Angular deformation vs. current for SSC

used with angular deformations measured at increasing intervals of 0.06 A from 0 to 0.24 A. The maximum angular deformation observed was 72.31°. The plot of Figure 5.3 shows the increasing

angular deformation of the SSC against increasing current. The voltage was held constant at 14 V, with measurements taken at increasing intervals of 0.1 A from 0.6 A to 1.1 A. The maximum angular deformation observed was 81.63°.

The plots showed asymmetry due to the accumulation of errors caused by a repetition of processes during manufacturing of the samples. For the SSC actuators, because the sample production were not automated and were completed manually from start to finish, the orientation of the clamped rings at the ends of the SMA wires were all different. Furthermore, the thickness of the PDMS matrix has proven to be difficult to control. Several factors play a role: different amounts of PDMS polymer gets absorbed by the PLA molds, irregularly filleted corners of the PLA mold during 3D printing cause different levels of surface tension of the poured PDMS, and more. During the manufacturing process of the IPMC, prolonged exposure of the samples in heated solutions with turbulence caused by the magnetic stirrer has produced several instances of samples with curvature. Additionally, the repeated coating processes have increased surface stiffness due to the aggregation of Pt particles, causing the curved samples to retain the deformed structure. The combination of the manufacturing errors played a collective role in causing the asymmetry of the deformation results in the plots.

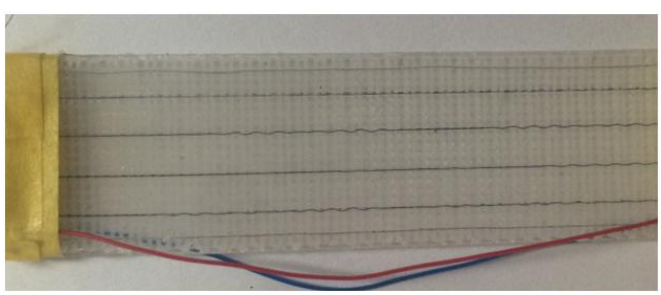

Figure 5.4 Warping of SMA wires in a used SSC actuator

Aside from the manufacturing errors, the actuators have also displayed signs of compromise in the integrity and durability after prolonged exposure to current. Figure 5.4 shows the curling of the

SMA wires within the PDMS matrix after prolonged, repeated use of the SSC sample. This was likely caused by the loosening of the PDMS grip on the embedded SMA wires after several operations. Another instance of the problems in durability was found in the IPMC, where prolonged exposure to a DC current have burned the interface between the actuator surface and the electrical wire extending to the voltage source. The exceptionally high voltage for operating the IPMC have caused the moisture content to deplete rapidly via electrolysis, causing the electrical wire to burn the surface at the interface.

5.2. Force and Resonance Frequency

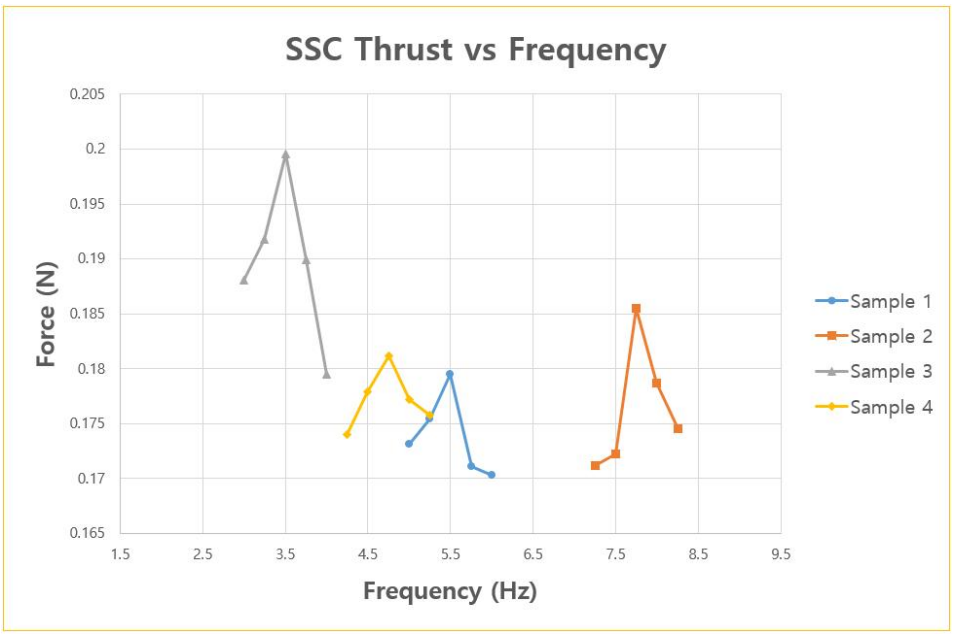

Figure 5.5 Thrust vs. frequency for SSC samples 1~4

To study the actuation force of the hybrid actuator, thrust was measured at various frequencies to determine the maximum force. The maximum force was found at resonance, when the angular deformation of the actuator was at its highest value. Figure 5.5 shows the maximum thrust of the samples 1~4, each occurring at

their corresponding resonance frequencies. For the samples with two SMA wires (samples 1 and 4), current was set at 0.4 A for operation. For samples with four SMA wires (samples 2 and 3), the current was set at 0.9 A.

The highest value of thrust was observed in sample 3, at 199.6 mN, most likely due to the high force density of having four SMA wires. The highest resonance frequency was observed in sample 2, at 7.75 Hz, most likely due to its shorter length and greater thickness caused by the thicker scaffold. With shorter length and a larger thickness, the frequency required to match the natural frequency is greater due to the increase in stiffness [28].

A potential error that may have occurred during the experiment may be the ambient mechanical vibrations from the work table. Because the jig holding the SSC actuator for the force test extends a significant vertical distance from the force sensor, small vibrations that may have been present on the work table - which may have originated from various equipment in use at the time for the experiment - could have amplified the thrust measurements.

5.3. Effects of Parameters on Performance

Table 4 shows the ranks by influence for each parameter of the Taguchi method on the performance of the SSC and hybrid actuator. The results show that the scaffold thickness has the greatest influence on the deformation of the actuator, and that the number of wires has the most influence on the value of the resonance frequency and thrust. With thinner scaffolds, there was less resistance by the PDMS to deformation, allowing for greater curvature of the actuator. The number of wires were directly related to the force density of the actuator, the increase of which translated to an increase in maximum thrust. The greater number of SMA wires also translated to a more drastic change in resonance frequency, as a significant spread of resonance frequencies was observed for samples with four SMA wires than those with two.

The length played a relatively important role at influencing the performance of the actuator, with an influence rank of 2 across all categories. Further tests can be done with a wider range of values for the parameters under examination. Alternatively, new parameters can be investigated for the effect on the performance. Using the influence chart as a reference, a hybrid actuator can be intentionally designed to emphasize a specific category. For instance, a soft robotic limb with low flexibility and high force density can be created with an emphasis on the number of wires by embedding more than four into the SSC component.

Table 4. Ranks of parameter influence on the performance of SSC and hybrid actuator

	Length	Scaffold thickness	Number of SMA wires
Deformation	2	1	3
Res. Freq.	2	3	1
Force	2	3	1

Chapter 6. Characteristic Changes by PWM

6.1. Premise

The results of the basic parametric studies in Chapter 5 have shown that angular deformation and thrust of SSC actuators are affected by the supplied voltage. According to Ohm's law, the current flowing through the circuit is directly proportional to the supplied voltage:

$$V = IR \tag{1}$$

Thus, it would be possible to achieve various levels of deformation and force by using some technique to actively adjust the voltage supplied to the actuator. One such method would be the Pulse Width Modulation (PWM) [27].

The crystalline structure within SMA wires changes based on the changes in temperature and stress [21]. Because the shape memory effect is "turned on and off" with the presence and absence of heat in the structure, DC currents were used to control the SMA wires on both sides of the actuator. For the same reason, the AC current was not considered for the manipulation of the wires, as the wires would be exposed to varying degrees of heat for a longer period of time, thus undergoing structural change beyond the desired duration of actuation. The integrity of the flapping motion of the SSC actuator would suffer due to the residue heat caused by slower heat dissipation in the crystalline structure. Therefore, the PWM method was implemented to transmit discrete inputs of current to effectively control the SSC actuator. The sudden introduction of current input quickly changed the martensitic state of the SMA wires into the austenitic, while the sudden absence allowed the heat to begin escaping the structure immediately. This particular technique allowed the SSC actuator to be actuated at high frequency in a flapping motion with lesser compromise to

performance, specifically force and speed, than were it be actuated with AC currents.

6.2. Effects of Variation in PWM

The SSC samples 1~4 were operated at different duty cycles to determine the effects on the deformation and resonance frequency. Figures 6.1, 6.2, and 6.3 each show the angular deformation plotted against frequency for all four samples at 25%, 50%, and 75% duty cycles, respectively. Tables 5 and 6 show the measured values of angular deformation and resonance frequency, respectively.

Across all samples, a general observation of maximum deformation and minimum resonance frequency can be made at 50% duty cycle. At low duty cycles, there is much more time between the input signals for the SMA wires to cool off than there would be for 75% duty cycle. The better heat dissipation rate allows the SSC actuators to operate well beyond its typical life cycle when operated at a higher duty cycle. However, the low duty cycle does not allow the heat to build up in the SMA wires long enough for the SSC actuators to deform effectively, resulting in low angular deformation. For 75% duty cycle, the samples built up heat in the SMA wires more quickly than they did for the 25% duty cycle, which led to a decrease in performance at prolonged operations. However, the longer exposure to heat allowed the SSC actuators to deform more completely than they did for the 25% duty cycle.

Between the high and low ends of the duty cycle values, the performance observed at 50% was observed to be the best. This is because high levels of deformation are synonymous with high levels of force, and deformation and force are generally the most sought after parameters to optimize in applications. The selection of duty cycle for the SSC actuator (and the hybrid actuator) operation can be situational. To increase the life time of the actuator and conserve energy by compromising performance, a low duty cycle value can be chosen. For peak performance, a higher value of duty cycle can

be chosen, which is observed to be around 50%. The repeated tests have shown that the optimal value of duty cycle that prioritizes performance over life time resides within the range of 50% to 75%.

Further tests can be done at smaller intervals of duty cycle, such as 20-40-60-80, to establish a better understanding of the behaviors of the SSC and hybrid actuators, and to determine the optimal duty cycle for various circumstances.

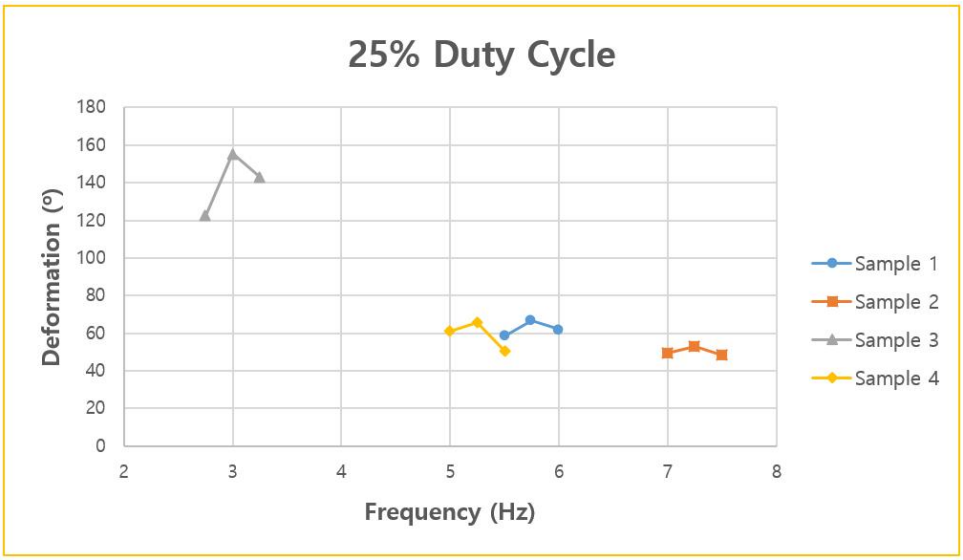

Figure 6.1 Angular deformation vs. frequency for 25% duty cycle

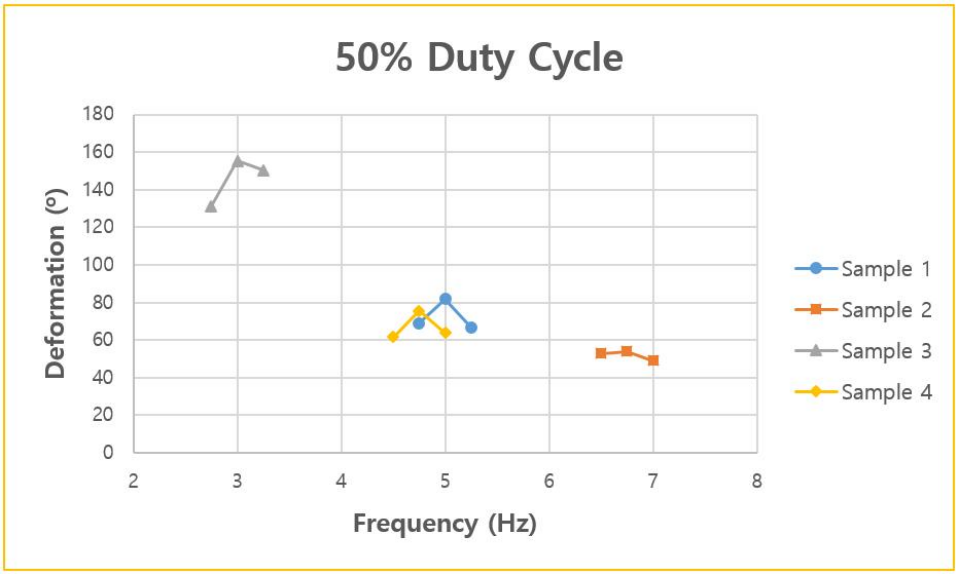

Figure 6.2 Angular deformation vs. frequency for 50% duty cycle

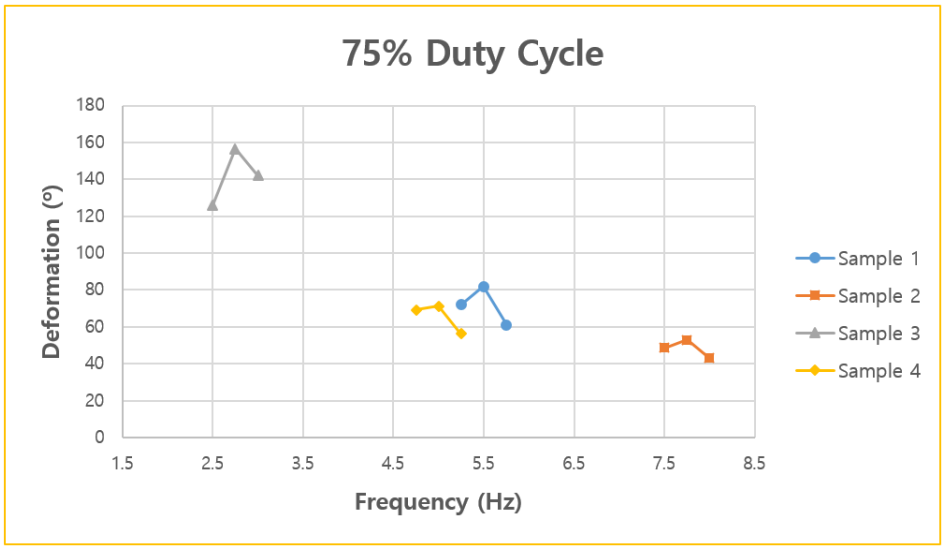

Figure 6.3 Angular deformation vs. frequency for 75% duty cycle

Table 5. Angular deformation of SSC samples under different duty cycles

	Sample 1	Sample 2	Sample 3	Sample 4
25%	66.8°	52.82°	155.44°	65.45°
50%	81.9°	53.87°	155.23°	75.53°
75%	81.87°	52.8°	156.44°	71.13°

Table 6. Resonance frequency of SSC samples under different duty cycles

	Sample 1	Sample 2	Sample 3	Sample 4
25%	5.75 Hz	7.25 Hz	3 Hz	5.25 Hz
50%	5 Hz	6.75 Hz	3 Hz	4.75 Hz
75%	5.5 Hz	8 Hz	2.75 Hz	5 Hz

Potential errors that may have affected the experiments may lie in the asymmetry of the actuation caused by the accumulative manufacturing errors mentioned in Chapter 5.

Chapter 7. Alteration of Resonance Frequency

7.1. Premise

In the previous chapters, the hybrid actuator performance was drawn from the behaviors of its main component, the SSC. Aside from the examination of general performance, a more direct effect of the IPMC actuation on the SSC characteristics was investigated. Considering the low force density of the IPMC component, it was deemed feasible to assess the effects on the resonance frequency rather than the overall force.

7.2. Effect on Resonance Frequency

To determine the effects on the resonance frequency, the resonance frequencies were measured for the SSC without IPMC and with IPMC actuating at its resonance frequency. It was plausible to surmise that due to its low force density, the IPMC may prove to have no influence on the resonance frequency of the SSC. Therefore, in order to validate the significance of using an IPMC over any other film-like object, a static compliant fin created from A4 paper with the same dimensions as the IPMC sample was used for the testing, as well. The IPMC was operated at resonance frequency during testing because it was capable of producing the greatest amount of deformation and force at resonance.

The results of the tests have shown that different characteristics could be observed for the three cases examined. Figure 7.1 shows the plot comparing the evident characteristic differences. SSC operated alone without the presence of IPMC had shown the greatest amount of angular deformation of 102.99° at a resonance frequency of 3.5 Hz. When the static compliant fin was added, the deformation dropped to 94.86° with no change in the resonance frequency. This was most likely due to the fin creating

drag to decrease the overall deformation of the SSC component.

When the IPMC component was added and operated at resonance, both deformation and resonance frequency of the SSC decreased. The deformation dropped to 88.35° at resonance frequency of 3.25 Hz. The minute effect of IPMC movement at the tip of the SSC, where IPMC influence can be maximized, had created a significant resistance in the movement of the SSC component, thereby decreasing both the angular deformation and frequency at which its resonance could occur.

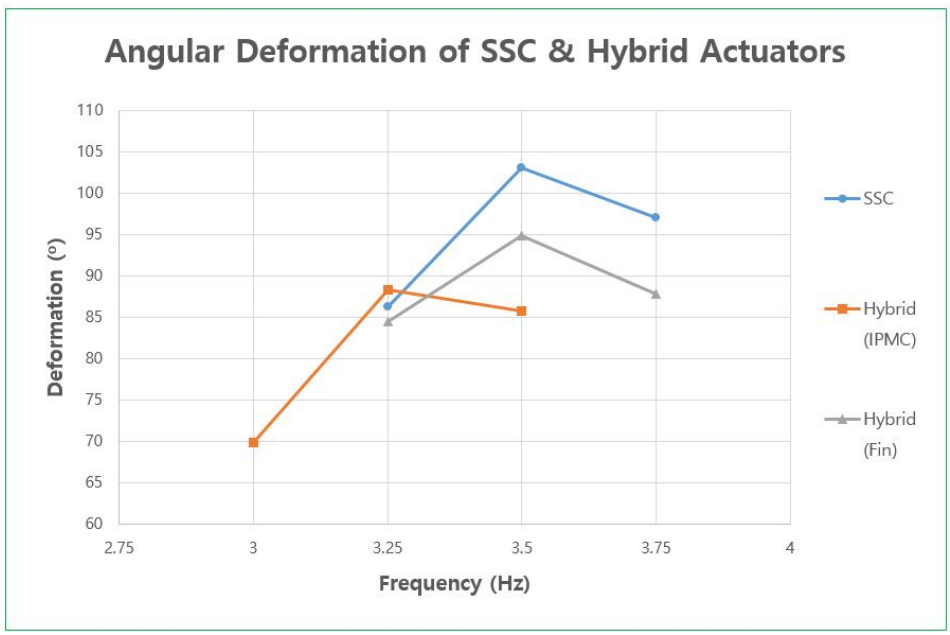

Figure 7.1 Comparison of resonance for SSC and hybrid actuators

The experiment can be further developed to confirm the validity of the generalization of the characteristic change in resonance frequency by extending the scenario to SSC components of various parametric values. Although for the scope of this research, the parameters of the IPMC actuator were held constant, IPMC samples of different dimensions and geometry can be tested for various effects on the resonance frequency. Once an optimal design is found, sufficient application can be proposed.

Chapter 8. Conclusion

The purpose of this research was to develop a hybrid actuator with two different smart materials. To the extent of author's knowledge, this work is the first documented instance of a hybrid actuator capable of various modes of actuation that relies on the direct contribution of two different smart materials with distinct actuation mechanisms. Although there have been some research in compound actuators that associate two different smart materials and/or actuation mechanisms, the author believes that the hybrid actuator in this study is unique in the sense that one smart material mechanically assists and alters the characteristics of another.

With the proposal of a new design of the SSC actuator to accommodate integration of two separate bodies, a hybrid actuator was created in serial configuration. The Taguchi's DOE was implemented to determine that scaffold thickness and number of SMA wires had the greatest impact on the performance of SSC, which had an analogous characteristic behavior to that of the hybrid actuator. Multiple modes of actuation were validated, controlled by various levels of current. Different duty cycles were tested to find that the optimal duty cycle for peak performance of the SSC and hybrid actuator was in the range of 50% to 75%. Lastly, IPMC at resonance was found to decrease deformation and resonance frequency of its complementary SSC component.

The hybrid actuator can be manufactured with careful control of parameters to accentuate different characteristics, which can be chosen strategically to create actuators for various situations. One potential application of the hybrid actuator is the biomimetic Swallowtail butterfly wing, with SSC as the wing and the IPMC as the wing tip [29]. Number of embedded SMA wires can be increased while decreasing scaffold thickness to create a lightweight wing with high force density. The IPMC wing tip can be designed to increase lift upon actuation. The design can be optimized further create a biomimetic soft robot that can not only

fly, but can also swim underwater.

Bibliography

1. Ma, K. Y., Chirarattananon, P., Fuller, S. B., & Wood, R. J. (2013). Controlled Flight of a Biologically Inspired, Insect-Scale Robot. Science, 340(6132), 603-607. doi:10.1126/science.1231806
2. Villanueva, A., Smith, C., & Priya, S. (2011). A biomimetic robotic jellyfish (Robojelly) actuated by shape memory alloy composite actuators. Bioinspiration & Biomimetics, 6(3), 036004. doi:10.1088/1748-3182/6/3/036004
3. Sunkara, V., Ye, Z., Chakravarthy, A., & Chen, Z. (2016). Collision avoidance by IPMC actuated robotic fish using the collision cone approach. 2016 IEEE International Conference on Simulation, Modeling, and Programming for Autonomous Robots (SIMPAR). doi:10.1109/simpar.2016.7862402
4. Ge, Q., Sakhaei, A. H., Lee, H., Dunn, C. K., Fang, N. X., & Dunn, M. L. (2016). Multimaterial 4D Printing with Tailorable Shape Memory Polymers. *Scientific Reports, 6*(1). doi:10.1038/srep31110
5. Zhou, Y., & Huang, W. M. (2015). Shape Memory Effect in Polymeric Materials: Mechanisms and Optimization. *Procedia IUTAM, 12*, 83-92. doi:10.1016/j.piutam.2014.12.010
6. Ochoa, M., Chitnis, G., & Ziaie, B. (2013). Laser-micromachined cellulose acetate adhesive tape as a low-cost smart material. *Journal of Polymer Science Part B: Polymer Physics, 51*(17), 1263-1267. doi:10.1002/polb.23337
7. Gladman, A. S., Matsumoto, E. A., Nuzzo, R. G., Mahadevan, L., & Lewis, J. A. (2016). Biomimetic 4D printing. Nature Materials, 15(4), 413-418. doi:10.1038/nmat4544
8. Ge, Q., Dunn, C. K., Qi, H. J., & Dunn, M. L. (2014). Active origami by 4D printing. Smart Materials and Structures, 23(9), 094007. doi:10.1088/0964-1726/23/9/094007

9. Tibbits S. (2014). 4D printing: Multi-material shape change.Architectural Design, 84(1), 116–121. 10.1002/ad.1710
10. Kim, T., Zhu, L., Al-Kaysi, R. O., & Bardeen, C. J. (2014). Organic Photomechanical Materials. ChemPhysChem, 15(3), 400-414. doi:10.1002/cphc.201300906
11. Uchino, K., & Nomura, S. (1981). New Electromechanical Materials and Their Applications. *Japanese Journal of Applied Physics, 20*(S4), 225. doi:10.7567/jjaps.20s4.225
12. Hosono, N., Kajitani, T., Fukushima, T., Ito, K., Sasaki, S., Takata, M., & Aida, T. (2010). Large-Area Three-Dimensional Molecular Ordering of a Polymer Brush by One-Step Processing. *Science, 330*(6005), 808-811. doi:10.1126/science.1195302
13. M. G. *Kuzyk, Polymer Fiber Optics: Materials, Physics, and Applications*, CRC Press, Taylor & Francis Group, Boca Raton (2007)
14. Guo, S., Li, M., Shi, L., & Mao, S. (2012). A smart actuator-based underwater microrobot with two motion attitudes. *2012 IEEE International Conference on Mechatronics and Automation*. doi:10.1109/icma.2012.6284388
15. Shi, L., Guo, S., Li, M., Mao, S., Xiao, N., Gao, B., . . . Asaka, K. (2012). A Novel Soft Biomimetic Microrobot with Two Motion Attitudes. *Sensors, 12*(12), 16732-16758. doi:10.3390/s121216732
16. Shintake, J., Rosset, S., Schubert, B., Floreano, D., & Shea, H. (2016). Polymer Actuators: Versatile Soft Grippers with Intrinsic Electroadhesion Based on Multifunctional Polymer Actuators (Adv. Mater. 2/2016). *Advanced Materials, 28*(2), 205-205. doi:10.1002/adma.201670008
17. Sirohi, J., & Chopra, I. (2003). Design and Development of a High Pumping Frequency Piezoelectric-Hydraulic Hybrid Actuator. Journal of Intelligent Material Systems and Structures, 14(3), 135-147.

doi:10.1177/1045389x03014003002
18. Su, J., Xu, T., Zhang, S., Shrout, T. R., & Zhang, Q. (2004). A Hybrid Actuation System Demonstrating Significantly Enhanced Electromechanical Performance (Rep. No. LAR-16698-1). doi:20040055982
19. Su, J., Xu, T., Zhang, S., Shrout, T. R., & Zhang, Q. (2004). An electroactive polymer-ceramic hybrid actuation system for enhanced electromechanical performance. Applied Physics Letters, 85(6), 1045-1047. doi:10.1063/1.1779341
20. Su, J., & Xu, T. (2005). A modified electroactive polymer-ceramic hybrid actuation system (HYBAS) for aerodynamic control applications. Smart Structures and Materials 2005: Electroactive Polymer Actuators and Devices (EAPAD). doi:10.1117/12.600020
21. Satoh, G. et al (2010). Annealing Effect on the Shape Memory Properties of Amorphous NiTi Thin Films. Journal of Manufacturing Science and Engineering. doi:10.1115/1.4002189
22. Fuentes, J. G., Gümpel, P., & Strittmatter, J. (2002). Phase Change Behavior of Nitinol Shape Memory Alloys. Advanced Engineering Materials, 4(7), 437-452. doi:10.1002/1527-2648(20020717)4:7<437::aid-adem437>3.0.co;2-8
23. Ahn, S. et al. Smart soft composite: An integrated 3D soft morphing structure using bend-twist coupling of anisotropic materials. International Journal of Precision Engineering and Manufacturing, 13(4), 631-634. doi:10.1007/s12541-012-0081-8 (2012)
24. Shahinpoor, M. (n.d.). Chapter 23. Ionic Polymer Metal Composites as Soft Biomimetic Robotic Artificial Muscles. Ionic Polymer Metal Composites (IPMCs) : Smart Multi-Functional Materials and Artificial Muscles, 341-363. doi:10.1039/9781782627234-00341
25. Shahinpoor, M., & Kim, K. J. (2001). Ionic polymer-metal composites: I. Fundamentals. Smart Materials and Structures, 10(4), 819-833. doi:10.1088/0964-1726/10/4/327

26. Kim, K. J., & Shahinpoor, M. (2003). Ionic polymer metal composites: II. Manufacturing techniques. Smart Materials and Structures, 12(1), 65–79. doi:10.1088/0964–1726/12/1/308
27. Sun J. (2012) Pulse–Width Modulation. In: Vasca F., Iannelli L. (eds) Dynamics and Control of Switched Electronic Systems. Advances in Industrial Control. Springer, London
28. Song, S., Lee, J., Rodrigue, H., Choi, I., Kang, Y. J., & Ahn, S. (2016). 35 Hz shape memory alloy actuator with bending–twisting mode. Scientific Reports, 6(1). doi:10.1038/srep21118
29. Srigrarom, S. (2014). On the Wing (Vol. 8, Issue 8, pp. 48–50, Rep.). ANSYS, INC.

국문초록

전통적인 로봇에 비한 소프트 로보틱의 가장 핵심적인 장점은 로봇의 팔로 부드럽고 복잡한 움직임을 구현할 수 있다는 것이다. 다양한 구동 메커니즘 중에서도, 특유한 성질을 지닌 지능 재료들을 통합하여 소프트 로봇 시스템 내에서 향상된 기동성과 상당한 무게 감소를 이루어 낼 수 있다. 통상적으로는 단일 재료 접근법을 이용하여 그 재료 특성을 강조하여 시스템에 활용하곤 하였다. 하지만 이에 지능 재료를 하나 더 추가함으로써 기존의 기능성을 바꿀 뿐 아니라, 시스템의 퍼포먼스도 향상 시킬 가능성이 존재한다.

이 연구에서는 형상기억합금(shape memory alloy) 기반의 지능형 연성 복합재(smart soft composite)와 이온성 고분자-금속 복합체(ionic polymer-metal composite)로 구성된 하이브리드 구동기를 설계 및 제작하였다. 두 개의 다른 재료로 만든 구동기를 직렬 배열 형태로 제작하였으며, 하나의 컴포넌트가 다른 파트의 작동을 보조하는 목적으로 설계하였다. 다구찌 실험계획법을 활용하여 하이브리드 구동기의 퍼포먼스에 영향을 미치는 다양한 파라미터를 테스트 하였다. 지능형 연성 복합재 구동기의 제어 방법론 중의 하나인 펄스 폭 변조(PWM)의 듀티 사이클을 다양한 값으로 설정함에 따르는 영향도 탐구하였다. 끝으로, 지능형 연성 복합재에 대한 이온성 고분자-금속 복합체의 보조적 역할의 직접적인 영향 역시 조사하였다.

주요어: 형상기억합금, 지능형 연성 복합재, 이온성 금속 복합재, 지능 재료, 소프트 로보틱스, 하이브리드 구동기

학번: 2016-20693